Optimization of internal heat exchangers for hydrogen storage tanks utilizing metal hydrides

Stephen L. Garrison[a,*]
Bruce J. Hardy[a]
Mikhail B. Gorbounov[b]
David A. Tamburello[a]
Claudio Corgnale[a]
Bart A. van Hassel[b]
Daniel A. Mosher[b]
Donald L. Anton[a]

[a] Savannah River National Laboratory, Savannah River Site, Aiken, SC, 29808, USA
[b] United Technology Research Center, 411 Silver Lane, East Hartford, CT, 06108, USA

[*] Corresponding Author. Tel.: 803-725-2404,
E-mail address: Stephen.Garrison@SRNL.doe.gov (Stephen L. Garrison)

Abstract

Two detailed, unit-cell models, a transverse fin design and a longitudinal fin design, of a combined hydride bed and heat exchanger are developed in COMSOL® Multiphysics incorporating and accounting for heat transfer and reaction kinetic limitations. MatLab® scripts for autonomous model generation are developed and incorporated into (1) a grid-based and (2) a systematic optimization routine based on the Nelder-Mead downhill simplex method to determine the geometrical parameters that lead to the optimal structure for each fin design that maximizes the hydrogen stored within the hydride.

The optimal designs for both the transverse and longitudinal fin designs point toward closely-spaced, small cooling fluid tubes. Under the hydrogen feed conditions studied (50 bar), a 25 times improvement or better in the hydrogen storage kinetics will be required to simultaneously meet the Department of Energy technical targets for gravimetric capacity and fill time. These models and methodology can be rapidly applied to other hydrogen storage materials, such as other metal hydrides or to cryoadsorbents, in future work.

Nomeclature

Variables and Constants:

C	*Molar concentration* (mol m^{-3})
C_p	*Isobaric heat capacity* (J kg^{-1} K^{-1})
ΔH_{rxn}	*Enthalpy of reaction* (kJ (mol H$_2$)$^{-1}$)
P	*Pressure* (bar)
Q	*Internal heat generation or dissipation rate* (W m^{-3})
R	*Ideal gas constant* (J mol^{-1} K^{-1})
T	*Temperature* (K)
$\hat{h}$	*Specific enthalpy* (J kg^{-1})
h	*Heat transfer coefficient* (W m^{-2} K^{-1})
k	*Thermal conductivity* (W m^{-1} K^{-1})
$\vec{n}$	*Outward surface normal vector*
$\bar{\mathbf{q}}$	*Heat flux* (W m^{-2})
t	*Time* (s)
$\hat{u}$	*Specific internal energy* (J kg^{-1})
$\bar{\mathbf{v}}$	*Mass-averaged velocity vector* (m s^{-1})
Δt_p	*Pressure ramp time* (s)
ε	*Void fraction* (unitless)
$\phi_{viscous}$	*Viscous heat generation rate* (W m^{-3})
ρ	*Density* (kg m^{-3})

Subscripts:

Al	*Aluminum*
H$_2$	*Hydrogen*
bed	*Effective or bulk property of the bed*
fill	*Filling*
fluid	*Cooling fluid*
inj	*Injection*
particle	*Particle*
res	*Resistive layer between (a) bed and (b) fin or tube*
wall	*Cooling tube wall*
1,2	*Ordinal label for reactions, surfaces, or domains*
0	*Initial*

1 Introduction

A key technical hurdle to an energy economy focused on clean-burning hydrogen over non-renewable petroleum is sufficient on-board storage of hydrogen for automotive vehicular applications. Automotive applications put significant requirements on the gravimetric and volumetric capacity of hydrogen storage systems since vehicle mass and fuel tank volume significantly affect vehicular fuel efficiency and available passenger and cargo space, respectively. As hydrogen is a low-density gas at ambient conditions, other techniques are required to store sufficient hydrogen in a small volume to satisfy consumer expectations for travel range and cargo and passenger space.

Metal hydrides provide one possible solution to the need for high gravimetric and volumetric capacities by storing hydrogen in a high density form, i.e., as a solid. For metal hydrides with sufficiently high weight fractions of reversibly stored hydrogen, fill times, i.e., uptake kinetics, become a dominant issue of concern. Metal hydrides release significant amounts of heat during hydrogen uptake, on the order of 20 MJ per kg of hydrogen, likely resulting in increased temperatures within the fuel tank, i.e., the hydride bed. While reaction kinetic rates generally increase as temperatures increase, the saturation pressure, i.e., the pressure below which the metal hydride is more stable as 'un-stored' hydrogen gas and metal hydride precursor, also rises. Unless the storage system and hydrogen feed pressures are correspondingly increased above the saturation pressure as the temperature increases, the storage of hydrogen as a metal hydride will stop due to the increased temperatures, which decreases the maximum hydrogen storage capacity of the hydride. If the temperature increases such that one or more the hydriding reactions reverses during the charging process, the metal hydride precursor in the storage tank serves no purpose as it occupies space in which additional hydrogen gas could be stored if the precursor was not present.

Given the fill times specified by the Department of Energy (DOE) technical targets[1], within the hydride bed, heat removal rates on the order of 0.1 MW per kg of reversibly stored hydrogen would be required to maintain the storage bed at or near optimum conditions to minimize fill times. Integrated tank heat exchangers, e.g., cooling tubes and fins, within the hydride bed are needed to maximize heat transfer out of system to maximize storage rate and capacity. The need to perform experiments safely, due to the possibility of high hydrogen feed pressures or water- or air-reactive chemicals, would make individual experiments extremely expensive. The range of bed designs, complex coupling of heat transfer, mass transfer, and chemical reaction kinetics within the hydride bed, and multiple metal hydride precursors of interest would necessitate an astronomical amount of time and money to design an optimal storage system via experiments.

The majority of studies in the literature on metal hydrides focus simply on their maximum reversible hydrogen capacity assuming an infinite fill time, which provides little information on applicability of a proposed metal hydride in real situations and system designs. On the other hand, detailed numerical models that couple heat and mass transfer and chemical reaction kinetics would provide a much more efficient approach than experiments to evaluate and optimize the design of the hydride bed to satisfy all of the DOE targets. Previous scoping[2] and detailed numerical modeling[3] indicate kinetics and thermal limitations within one proposed metal hydride, sodium alanate (NaAlH$_4$), that likely also apply to other metal hydrides. Therefore, optimization of the storage tank and placement of the integrated heat exchanger elements is needed to maximize capacity while minimizing fill time

2 Background

Mellouli, et al. analyzed three variations of a metal hydride based storage system originally described in [4], using a 2-dimensional (r-z) numerical model they developed [5]. In particular, the model was employed to evaluate various methods of heat exchange for the vessel. The 2-dimensional equations defining the model were solved using the control volume finite element method. The storage vessel was a cylinder that confined the metal hydride to a cylindrical geometry and was cooled by combinations of: a water

jacket, a helical cooling tube embedded in the metal hydride with water used as the heat transfer fluid, and natural convection[5]. Mellouli applied the model to the charging phase for a $LaNi_5$ based system[5] and used the hydrogen loading rate as the criterion for ranking the storage vessel performance. Mellouli, et al. then applied the model to a coupled system of two helical coil cooled storage vessels to evaluate using uptake and discharge heats of reaction to improve the efficiency of the charging process[6]. In that study the storage media was $MmNi_{4.5}Al_{0.4}/MmNi_{4.2}Al_{0.1}Fe_{0.7}$ (where Mm is mischmetal or "mixed metal") and the evaluation was based on the coefficient of performance. Mellouli, et al. also applied their 2-dimensional model[4] to a cylindrical storage vessel using $LaNi_5$ as a storage media[7]. Heat exchanger designs evaluated in this study consisted of a central coolant tube embedded in the media, a finned central tube, a vessel without a coolant tube and finned radial wall that transferred heat to the ambient and a vessel with no coolant tube and without external fins on the radial wall. Temperature profiles and hydrogen charging rates were used to evaluate the effect of fin diameter and material composition (brass or steel). Because the thermal conductivity of brass or steel greatly exceeds that of the bed, the study indicated that there was no difference in the hydrogen charging rate for either type of fin. Mellouli, et al. again applied their 2-dimensional model[4] to modifications of their heat exchanger design[5], using $LaNi_5$ as the storage media[8]. Heat exchanger modifications included fins and concentric coils. Optimization, based on the hydrogen charging rate, was performed for the spacing, length and thickness of the fins. As with prior studies by Mellouli, et al., the optimization process consisted of varying of the aforementioned parameters until the increase in the loading rate became sufficiently small.

Kikkinides, et al. developed a 2-dimensional (r,z) model for a metal hydride storage vessel having a heat exchanger in the form of an annular ring, with some designs having a central tube[9-10]. The storage media used in the vessel was $LaNi_5$. The geometry of this system makes the heat transfer design similar in some regards to the helical coil heat exchanger of Mellouli, et al.[5]. The Kikkinides, et al. model employed gPROMS as the equation solver. Control vector parameterization, within gPROMS, was used to optimize the system design (radius of the annular cooling ring as well as the use of a central coolant tube) and operating strategy, again based on the hydrogen charging rate.

MacDonald and Rowe developed models to investigate the impact of external convection on desorption of hydrogen from a cylindrical $LaNi_5$ based storage vessel[11]. A 1-dimensional steady-state resistive model and a 2-dimensional transient model, based on FEMLAB® were used to evaluate storage system performance. In this paper a cylindrical storage vessel with no internal heat transfer structures, with and without external fins, was examined. Hydrogen discharge from the storage vessel was thus effected by exposing the exterior of the storage vessel to the ambient temperature, assumed to be 25°C in this study. Pulsed hydrogen discharge, corresponding to the hydrogen flow demands of a fuel cell, was considered for vessels that were initially full and 2/3 full.

Mohan, et al. developed a 2-dimensional (r,θ) model for the cross-section of a cylindrical $LaNi_5$-based hydrogen storage vessel with multiple coolant and injection tubes passing axially through the bed[12]. The model, developed in COMSOL® was used to optimize the loading rate of the storage vessel by varying the spacing between the outer

surface of the coolant tubes, the ratio of the coolant tube radius to the center-to-center tube spacing and the coolant tube diameter. In the optimization process, these parameters were varied until the change in the loading rate became sufficiently small. It was found that the charging rate was most sensitive to the spacing between the outer surface of the coolant tubes, and to a lesser extent on the ratio of the coolant tube radius to the center-to-center tube spacing.

In this work, we model the coupled heat and mass transfer of a sodium alanate complex metal hydride bed as it uptakes hydrogen. The model is developed in COMSOL® and linked to optimization routines within Matlab® to study the ability to optimize the system to maximize the gravimetric capacity of the metal hydride (included the mass of the integrated heat exchanger) neglecting the hydrogen stored in the porous, gas-phase portion of the packed bed. To match with previous work[3], the hydrogen fill pressure was set to 50 bar and the fill time was set to 12 minutes, which is significantly longer than the DOE target of 4-5 minutes. The number of unit cells required to store 1 kg of hydrogen within the media given these conditions was then calculated. From this a gravimetric capacity was calculated based on the hydrogen stored versus the mass of the integrated heat exchanger and the hydride media. This value for gravimetric capacity was the optimization variable that was maximized within the optimization routines by minimizing the combined mass of the integrated heat exchanger and the hydride media. A manual, grid-based, optimization was completed first and the result subsequently used in a automated, Nelder-Mead downhill simplex optimization.

3 Methodology

The underlying physics included within the model are comprised of two components: (1) reaction kinetics for the reaction of hydrogen and the metal hydride precursor to (or from) the metal hydride, and (2) energy transfer (as heat) from the hydride bed to the integrated heat exchanger components (the cooling fins and coolant tubes). In contrast to previous models, mass transfer resistance of the hydrogen flowing through the bed was neglected, i.e., the bed pressure was assumed to be spatially uniform or homogenous throughout the bed. This was done to simplify the model to speed the optimizations and was validated by the observation that the spatial gradients in pressure were extremely small for the full models that were tested, but not reported. The reaction kinetics and energy transfer of the system are intricately linked as the local bed temperatures control the rates and direction of the hydriding/dehydriding reactions, the rates and direction of the reactions control the heat generated or consumed, and the ability to distribute the heat generated from the bed to the cooling fins and coolant tubes controls the local bed temperatures.

3.1 Assumptions

A number of simplifying assumptions are made in the model to facilitate the modeling of the overall system. They are as follows:

1   The instantaneous gas pressure is homogenous throughout the bed meaning that mass transfer limitations and viscous flow resistances are neglected. Given the small pressure gradients in the previous model[3] this is a reasonable approximation. However, the system pressure is allowed to change as a function

of time to model an initial ramp up in the bed pressure as it is connected to a hydrogen refueling source.

2 The bed void fraction remains constant and uniform throughout.

3 The density of the bed does not change as a function of time, temperature, or composition, i.e., the bed does not expand or contract as a function of the amount of hydrogen loading or temperature. This assumption is especially significant because all materials proposed for hydrogen storage undergo significant expansion during hydrogen loading.

4 The thermal properties of the bed do not change as a function of time, temperature, or composition, i.e., the heat capacity and thermal conductivity of the bed do not change as a function of the hydrogen loading or temperature.

5 The characteristics, e.g., the kinetics and thermal properties, of the bed are unaffected by the number of loading-unloading cycles. That is, bed aging is neglected.

6 At each location within the bed, the solid phase and the hydrogen gas have the same instantaneous temperature. However, the temperature is not homogenous throughout the bed.

7 Overall heat transfer out of or into the bed occurs only via the heat transfer fluid (in the cooling tubes) and by homogeneous heat exchange with the gaseous hydrogen in the bed.

8 The thermal conductivity, specific heat and viscosity of hydrogen do not vary with pressure over the operational regime of the storage system.

9 For this system, the equation of state for hydrogen is given by the ideal gas law.

10 The tubes and fins are composed of 6063 T83 aluminum, the thermal properties of which are provide by internal libraries within COMSOL®.

11 The independent area around each cooling tubes is assumed to be circular. This assumption is most valid for multiple cooling tubes tiled in a hexagonal fashion.

12 Thermal contact resistance between (1) the bed and the cooling tubes and (2) the bed and the fin is modeled by a thin, resistive layer with thermal conductivity of 5e-4 $W \cdot m^{-1} \cdot K^{-1}$ and thickness 1e-6 m, yielding an effective heat transfer coefficient of 500 $W\ m^{-2}\ K^{-1}$, which correlates well with the worst case thermal contact resistance found in previous research [13]. Thermal contact between the fin and the cooling tubes is good, i.e. thermal contact resistance between the fin and cooling tube is neglected.

13 The bed fills the entire volume of the space between the fins and tubes.

14 The bulk temperature of the cooling fluid is constant and uniform. Sufficient mass of cooling fluid is assumed to be moving through the cooling tubes and the axial length of the cooling tubes is assumed to be sufficiently short that the heat absorbed from or released to the bed results in negligible temperature change of the cooling fluid. Additionally, regardless of tube diameter or assumed cooling fluid flow rate, the heat transfer coefficient is assumed constant at 1500 $W\ m^2\ K^1$.

15 Axial end-effects have negligible impact on the performance of the storage system.

16 Hydrogen is assumed to follow the ideal gas equation of state such that its molar concentration is defined by the pressure and temperature, in the form of Eq. 1.

$$C_{H_2} = {P_{H_2}}\big/{RT} \tag{1}$$

17. The amount of hydrogen stored in the gas phase within the pores is currently neglected when computing the total amount of stored hydrogen. As the system pressures and bed void volumes are constant, this term would be an additive constant to the total hydrogen stored. As such, it would affect the total hydrogen but will not affect the relative results for different geometries simulated.

18. The calculated mass of the system that is minimized corresponds to the mass of the cooling tubes, cooling fins, and metal hydride precursor material. The mass of the pressure vessel, the cooling fluid, and any balance of plant is currently neglected. Unless the total volume or surface area of the pressure vessel changes significantly as a function of the model geometry, the variability in the ignored mass should be negligible.

3.2 Storage Tank Governing Equations

The governing equations representing the underlying physics for the bed are comprised of two components: (1) the reaction kinetics for the reaction of hydrogen and the metal hydride precursor to (or from) the metal hydride with the corresponding heat generation (or consumption), and (2) the energy transfer (as heat) from the hydride bed to the integrated heat exchanger components (the cooling fins and coolant tubes).

3.2.1 Bed Energy Balance

The starting point for the bed energy balance is Eq. 2 (the energy conservation equation).

$$\rho \frac{D\hat{u}}{Dt} + P(\nabla \cdot \vec{\mathbf{v}}) = Q - \nabla \cdot \vec{\mathbf{q}} + \phi_{viscous} \tag{2}$$

By, neglecting the viscous heating terms, assuming Fourier's law of conduction, using the continuity equation, and relating the internal energy to the enthalpy via Eq. 3 we arrive at Eq. 4.

$$\hat{u} = \hat{h} - \frac{P}{\rho} \tag{3}$$

$$\rho \frac{D\hat{h}}{Dt} = \frac{DP}{Dt} + Q + \nabla \cdot (k\nabla T) \tag{4}$$

The enthalpy derivative can be expanded in terms of temperature and pressure via Eq. 5.

$$\frac{D\hat{h}}{Dt} = C_p \frac{DT}{Dt} + \left(\frac{1}{\rho} + \frac{T}{\rho^2} \frac{\partial \rho}{\partial T} \right) \frac{DP}{Dt} \tag{5}$$

Substituting Eq. 5 into Eq. 4, expanding the substantial derivative, and rearranging and collecting terms, Eq. 6 is obtained.

$$\rho C_p \left(\frac{\partial T}{\partial t} + \vec{\mathbf{v}} \cdot \nabla T \right) - \nabla \cdot (k\nabla T) = -\frac{T}{\rho} \frac{\partial \rho}{\partial T} \left(\frac{\partial P}{\partial t} + \vec{\mathbf{v}} \cdot \nabla P \right) + Q \tag{6}$$

Assuming a lumped model for the heat source and the conduction heat transfer (i.e., k is replaced by k_{bed} that accounts for all heat conduction in the bed through both the solid and gas phases), assuming a homogenous pressure everywhere thereby neglecting the convective (flow) terms, and splitting the temperature and pressure terms into their gas phase and solid phase components, Eq. 7 is obtained.

$$(1-\varepsilon)\rho_{particle}C_{p,particle}\frac{\partial T}{\partial t}+\varepsilon\rho_{H_2}C_{p,H_2}\frac{\partial T}{\partial t}-\nabla\cdot(k_{eff}\nabla T)=$$
$$-(1-\varepsilon)\frac{T}{\rho_{particle}}\frac{\partial\rho_{particle}}{\partial T}\frac{\partial P}{\partial t}-\varepsilon\frac{T}{\rho_{H_2}}\frac{\partial\rho_{H_2}}{\partial T}\frac{\partial P}{\partial t}+Q \tag{7}$$

If we assume the heat capacity and particle density are constant during the hydriding and dehydriding processes, assume no pressure work on the solid phase, and realize that $-\frac{T}{\rho}\frac{\partial\rho}{\partial T}=1$ for an ideal gas (Assumption 16), Eq. 8 is obtained.

$$\left((1-\varepsilon)\rho_{particle}C_{p,particle}+\varepsilon\rho_{gas}C_{p,gas}\right)\frac{\partial T}{\partial t}-\nabla\cdot(k_{eff}\nabla T)=\varepsilon\frac{\partial P}{\partial t}+Q \tag{8}$$

This assumes that, at any given location, the hydrogen contained within the voids of the bed and the solid material of the bed have the same instantaneous temperature, i.e., the solid and gas phases of the bed are assumed locally homogeneous in terms of temperature (Assumption 6).

The entire system (bed, fins, and cooling tube) are assumed to be at 100 °C initially. The boundary conditions for the energy balance are follows:

1. $\vec{n}\cdot(k\nabla T)=h_{cool}(T_{fluid}-T_{wall})$ for the interior surface of the cooling tube wall. (Heat flux boundary condition)

2. $\vec{n}\cdot(k\nabla T)=0$ for all other exterior boundaries. (Thermal insulation or symmetry boundary condition)

3. $\vec{n}\cdot(k_1\nabla T_1-k_2\nabla T_2)=0$ for all fin-fin, fin-tube, and tube-tube interior boundaries. (Continuity boundary condition)

4. $\vec{n}\cdot(k\nabla T_1)=\frac{k_{res}}{d_{res}}(T_2-T_1)$ and $\vec{n}\cdot(k\nabla T_2)=\frac{k_{res}}{d_{res}}(T_1-T_2)$ for interior boundaries between the media and either the tube or the fins. (Thin, thermally-resistive layer boundary condition)

3.2.2 Reaction Kinetics from UTRC

The reaction kinetics depend on the material used as the bed storage media. The kinetics equations are cast as a separate module within the set of governing equations defined in COMSOL Multiphysics® to permit them to be easily modified so that the model can be adapted to different metal hydride precursors, catalysts, or operating conditions. The current model uses an empirical kinetics model provided by United Technologies Research Center (UTRC) for the reaction of sodium hydride, NaH,

(Species 3) and aluminum metal, Al, catalyzed with 4% $TiCl_3$ to produce sodium alanate, $NaAlH_4$, (Species 1) as the final hydrogen storage material (metal hydride)[3; 13].

$$\underbrace{NaAlH_4}_{Species 1} \underset{Reaction 1}{\leftrightarrow} \underbrace{\frac{1}{3}Na_3AlH_6 + \frac{2}{3}Al + H_2}_{Species 2} \underset{Reaction 2}{\leftrightarrow} \underbrace{NaH}_{Species 3} + Al + \frac{3}{2}H_2 \qquad (9)$$
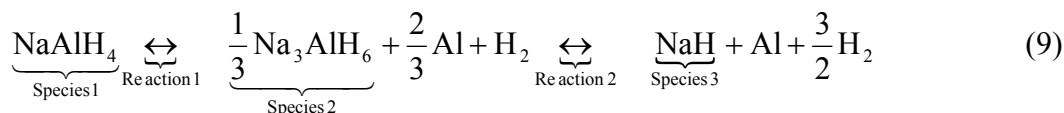
The enthalpies of reaction determine the heat released (or absorbed) during the uptake (or release) of hydrogen. For sodium alanate, under the convention that ΔH is negative for exothermic (i.e., heat generating) reactions, the heat generation term in the energy balance is:

$$Q = -\frac{dC_1}{dt}\Delta H_{rxn\,1} + 0.5\frac{dC_3}{dt}\Delta H_{rxn\,2} \qquad (10)$$

where, C_i is the concentration of species i and

$\Delta H_{rxn,1}$ = Enthalpy per mole of H_2 consumed for Reaction 1 going from Species 2 to Species 1
$\qquad$ = -37 kJ/(mole H_2 consumed)[13-15]
$\Delta H_{rxn,2}$ = Enthalpy per mole of H_2 consumed for Reaction 2 going from Species 3 to Species 2
$\qquad$ = -47 kJ/(mole H_2 consumed)[13-15]

Initially, the hydrogen pressure is 1 bar and the bed is assumed to be composed solely of hydride precursor materials with no $NaAlH_4$ or Na_3AlH_6 present. Although this does not consist of a steady state situation, it was assumed to be a reasonable initial condition. The boundary conditions for the reaction kinetics were insulated, or no flux, boundary conditions and the reaction only took place within the media portion of the bed and not within the cooling tube wall or fins.

3.3 Tank Design Models

Two designs for the coolant tube and cooling fin geometry were considered. The first design studied is that of a radial fin design, a common heat exchanger design more correctly referred to as a transverse fin design where the cooling fin is oriented transverse or perpendicular to the long or flow axis of the coolant tube. (See Figure 1a.) The second design studied is that of a longitudinal fin design where the cooling fin is oriented parallel to the flow axis of the coolant tube. (See Figure 1b.)
For both designs, a unit cell model was adopted to simplify the calculations. This assumes that end effects are negligible and that the temperature of the cooling fluid does not change as a function of axial position within the bed. The only other assumption required for the unit cell model to be reasonable is that each cooling tube within the bed is independent from all other cooling tubes. If the number of cooling tubes is large relative to the distance between cooling tubes, each tube sees its surroundings as an infinite sheet of cooling tubes; the boundary condition between the tubes then corresponds to a symmetry boundary condition of zero flux. This zero-flux boundary

(a)
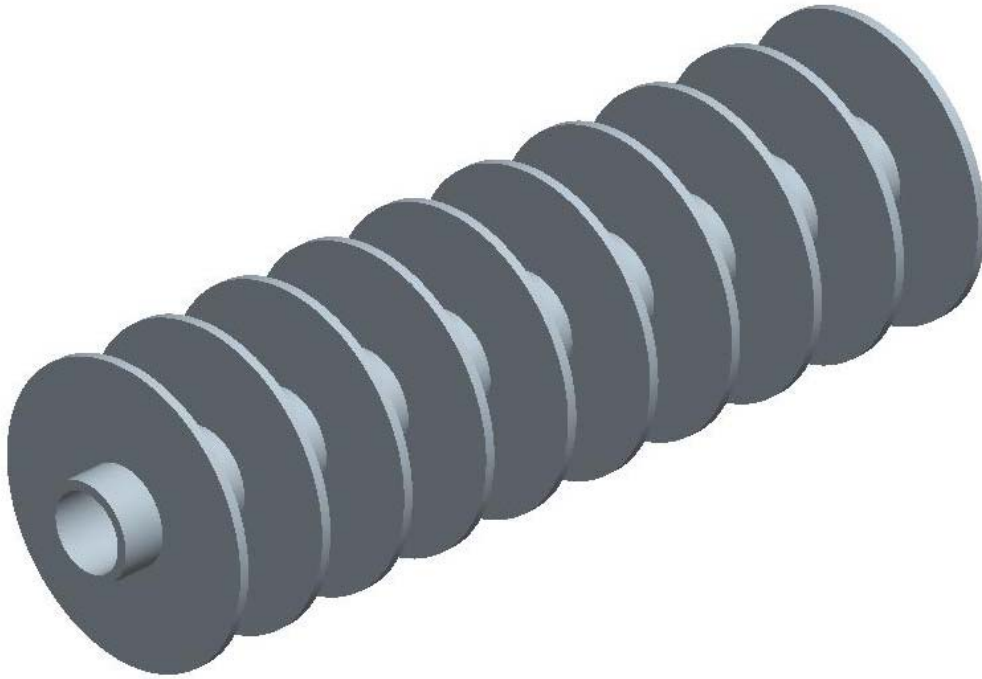
(b)
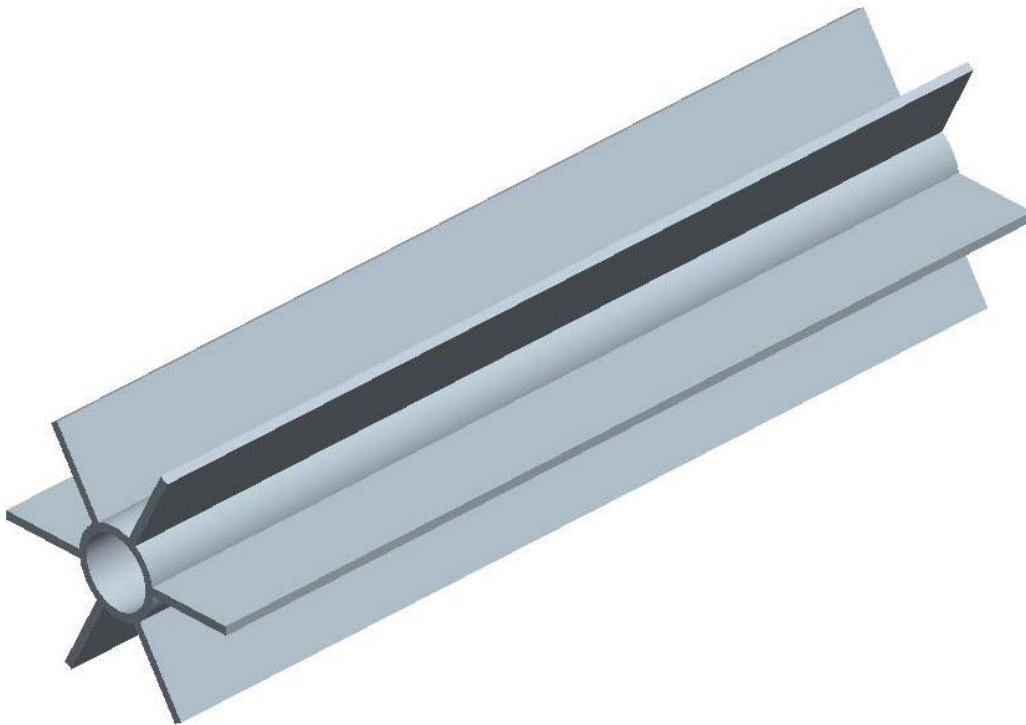
Figure 1: Heat exchanger designs: (a) transverse cooling fins; (b) longitudinal cooling fins.

SRNL-STI-2011-00424

(a)

(b)
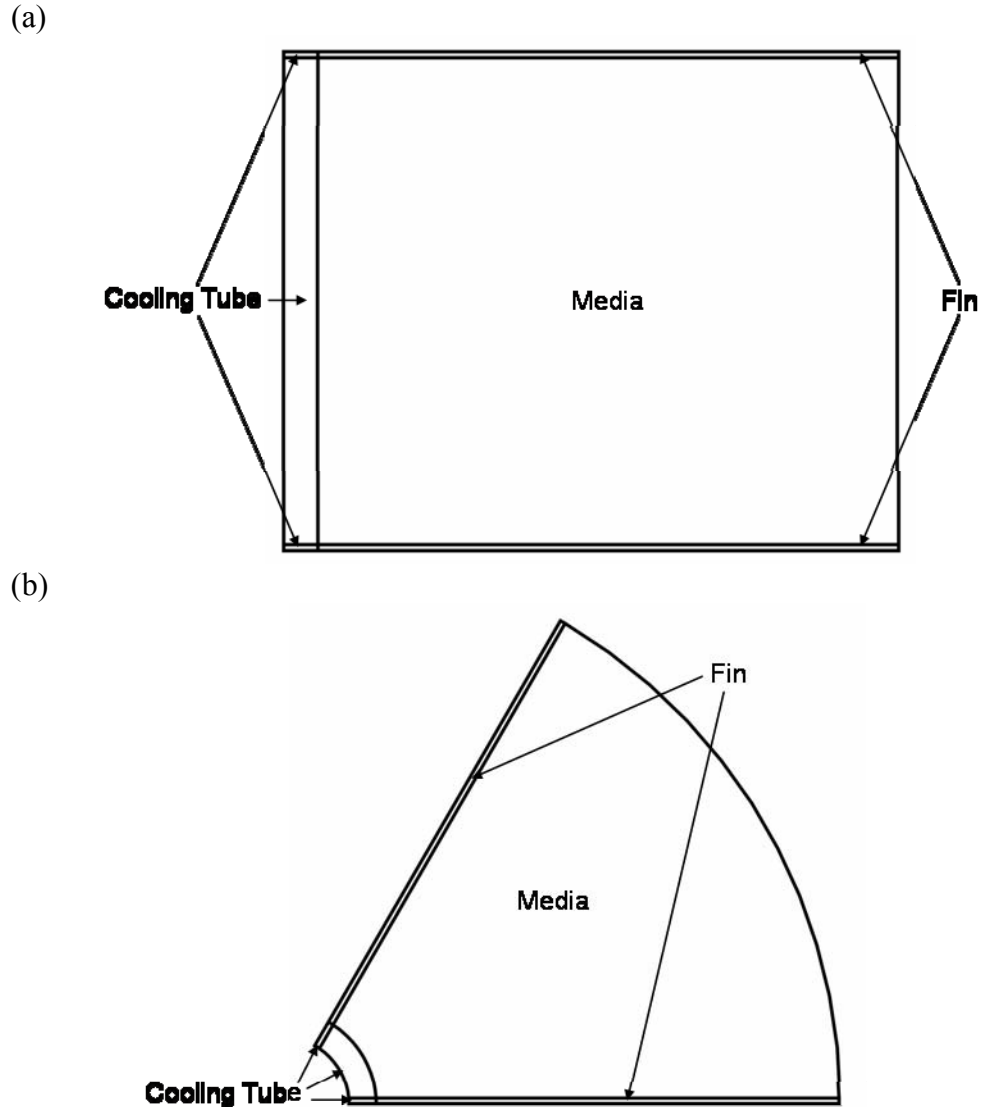
Figure 2: Heat exchanger unit cell models: (a) transverse cooling fins; (b) longitudinal cooling fins.

condition is mathematically equivalent to a perfect insulation boundary condition for heat transfer.

3.3.1 Transverse Cooling Fins

The model of the transverse cooling fin was generated as a 2-dimensional (2-D) axisymmetric (r-z) model, as seen in Figure 2a. The components explicitly modeled are the bottom half of the top fin, the hydrogen storage media, the top half of the bottom fin, and the cooling tube (as three subdomains). If the thermal contact resistances between (a) the top fin and the media and (b) the bottom fin and the media are identical (including the case where both thermal contact resistances can be neglected), then the model could be simplified to include only half of one fin and half of the media as the middle of the media would correspond to a symmetry, or zero-flux, boundary condition. However, both halves of both fins were included in the model in case one wanted to model the hydride media

resistances between the media and the two fins. The temperatures at the centerlines of the top and bottom fins were constrained to be identical as this must be the case for a unit cell model. This model could be viewed as similar to the model previously developed of UTRC Prototype 2[3].

3.3.2 Longitudinal Cooling Fins

The transverse fin design as the integrated heat exchanger in a metal hydride storage system suffers from two deficiencies. First, if the metal hydride storage tank is comprised of the integrated heat exchanger enclosed in an insulated pressure vessel, it will be difficult to pack the hydride precursor material densely between the cooling fins (to maximize the volumetric and gravimetric hydrogen storage densities) in an automated fashion (which will be required to produce storage tanks quickly and at reasonable cost) while maintaining good thermal contact between the cooling fins and coolant tubes while. A longitudinal fin design for the integrated heat exchanger could alleviate this issue and allow for mechanical compaction of the precursor material in an automated fashion. Second, a transverse fin design suffers from a decreasing cross-sectional area for heat flux as one moves from the fin tips to the coolant tube, possibly resulting in a bottleneck for heat transfer. Longitudinal fins maintain a constant heat transfer cross-sectional area as a function of the distance to the cooling tube. An additional benefit of the longitudinal fins is that they may also provide some structural support between cooling tubes to handle stresses generated by the hydrogen storage media expanding or contracting during hydriding and dehydriding. However, the maximum distance between two cooling fins attached to the same coolant tube increases as the distance between the cooling tubes increases, since the angular spacing is fixed.

The model of the longitudinal cooling fin was generated as a 2-D (x-y or r-θ) model, as seen in Figure 2b, that corresponds to a 60° slice of the area around one cooling tube. Thus, the model represents 1/6th of a full unit cell. The components explicitly modeled are the right half of the left fin, the hydrogen storage media, the left half of the right fin, and the cooling tube (as three subdomains). The centerlines of the left and right fins are 60° apart, with the centerline of the right fin corresponding to 0°, the centerline of left fin corresponding to 60°, and the centerline of the media corresponding to 30°. If the thermal contact resistances between (a) the left fin and the media and (b) the right fin and the media are identical (including both identical to zero), then the model could be simplified to include only half of one fin and half of the media as the middle of the media would correspond to a symmetry, or zero-flux, boundary condition. However, both halves of both fins were included in the model in case one wanted to model the hydride media pulling away asymmetrically from the fins, i.e., settling, yielding different contact resistances between the media and the two fins. The temperatures at the centerlines of the left and right fins were constrained to be identical as this must be the case for a unit cell model.

3.4 Model specifications

Table 1 gives the values used for the thermophysical properties of the materials within the model. The heat capacity of the gaseous hydrogen is given by Eq (11).

$$C_{p,H_2} = 11240.1 + 21.7312 \cdot T - 5.37450 \cdot 10^{-2} \cdot T^2 + 5.80853 \cdot 10^{-5} \cdot T^3 - 2.26488 \cdot 10^{-8} \cdot T^4$$
(11)

Table 1: Variable specifications within the models.

Variable	Description	Value	Units
$C_{1,0}$	Initial concentration of Species 1 (NaAlH$_4$)	0.0	mol m^{-3}
$C_{2,0}$	Initial concentration of Species 2 (Na$_3$AlH$_6$)	0.0	mol m^{-3}
$C_{3,0}$	Initial concentration of Species 3 (NaH)	13333.33	mol m^{-3}
T_0	Initial temperature	373.15	K
P_0	Initial pressure	1	bar
P_{inj}	Final H$_2$ feed pressure	50	bar
Δt_p	Time for system pressure (P) to go from P$_0$ to P$_{inj}$	10	s
T_{fluid}	Cooling fluid temperature	373.15	K
h_{fluid}	Heat transfer coefficient from coolant tube wall to coolant fluid	1500	W m^{-2} K^{-1}
t_{fill}	Time to charge media with hydrogen	720	s
$k_{res,}$	Thermal conductivity of thin, thermally-resistive layer between the media and either a cooling fin or tube	5e-4	W m^{-1} K^{-1}
d_{res}	Thickness of thin, thermally-resistive layer between the media and either a cooling fin or tube	1e-6	m
ε	Bed porosity or void fraction	0.5	(unitless)
$\rho_{particle}$	Media particle density	1440	kg m^{-3}
$C_{p,particle}$	Particle heat capacity	820	J kg^{-1} K^{-1}
k_{eff}	Bed effective thermal conductivity	0.325	W m^{-1} K^{-1}
ρ_{Al}	Aluminum density	2700	kg m^{-3}
$C_{p,Al}$	Aluminum heat capacity	900	J kg^{-1} K^{-1}
k_{Al}	Aluminum thermal conductivity	201	W m^{-1} K^{-1}
$\Delta H_{rxn\,1}$	Enthalpy of reaction for reaction 1 going from Species 2 to Species 1	-37	kJ (mol H$_2$)$^{-1}$
$\Delta H_{rxn\,2}$	Enthalpy of reaction for reaction 2 going from Species 3 to Species 2	-47	kJ (mol H$_2$)$^{-1}$

3.5 MatLab® Scripts for the COMSOL® Models

3.5.1 Optimization Parameters

The input parameters for the MatLab® scripts that generate and run the COMSOL® models are comprised of the following: (1) the inner diameter of the cooling tube, (2) the thickness of the cooling tube, (3) the length of the cooling fin, (4) the thickness of the cooling fin, and (5) the fin-to-fin centerline spacing. The fin-to-fin spacing is only a parameter for the transverse fin model. For the longitudinal fin model the fin-to-fin centerline spacing is fixed at 60°.

As the heat transfer coefficient between the cooling tube and the cooling fluid (h_{cool}) and the temperature of the cooling fluid are both assumed fixed and constant for all geometries, the inner diameter of the cooling tube is likely constrained solely by the need for sufficient surface area to yield the required heat flux given the heat transfer coefficient and the difference in temperature between the cooling tube inner wall and the cooling fluid. As such, the optimal value of this parameter is likely to always be at its minimum allowed value. However, if some of the assumptions in the models developed were removed, a smaller internal diameter would yield faster fluid flow and a higher heat transfer coefficient at the detriment of the total mass flow of coolant past each unit cell such that the axially isothermal assumption of the coolant (Assumption 14) may not be reasonable. Additionally, smaller cooling tubes could lead to unacceptably larger pressure drops, pointing to the appropriateness of a constrained minimum cooling tube diameter.

The combination of the cooling tube inner diameter and the cooling tube wall thickness control the outer diameter of the cooling tube. So long as the outer diameter of the cooling tube provides sufficient area for heat transfer area from the media and the fins to the cooling tube (and onward to the cooling fluid), optimization of this parameter will likely also point towards its minimum allowed value as that will help minimize the mass of the integrated heat exchanger by minimizing the volume of the cooling tubes, which are denser than the media. Smaller thicknesses also lead to shorter heat transfer distances, likely maximizing the heat flux. However, machineability and mechanical stability under the stresses of applied H_2 pressure, hydrogen loading and unloading, and vibration while in automotive use will mandate some minimum cooling tube thickness.

The combination of the fin length, the cooling tube inner diameter, and the cooling tube thickness specifies the spacing between cooling tubes once the unit cell design modeled here is extrapolated to a full tank design. While smaller fin lengths result in a shorter heat transfer distances from the media to the cooling tubes, it also increases the total number of tubes required given that there is a minimum amount of hydride precursor material necessary to store 1 kg of hydrogen even under an ideal heat transfer (isothermal bed) assumption. A larger spacing between cooling tubes should minimize the heat exchange mass and be easier to mechanically manufacture and assemble.

As long as there is sufficient cross-sectional area for the required heat transfer, the optimization routine will likely attempt to drive the fin thickness to a minimum value. Therefore, a minimum fin thickness was specified as a thinner fin would be unlikely to have sufficient mechanical stability to withstand the applied stresses during the assembly of the storage vessel and packing of the hydride precursor within it.

Similarly, it is probable that the optimization routine would point towards smaller and smaller centerline fin-fin spacing as this would minimize the heat transfer distance. However, if a minimum fin thickness is specified as described earlier, there should be a point at which closer fin-fin spacing is actually detrimental to the total mass of the system given that there is a minimum amount of hydride precursor material necessary to store 1 kg of hydrogen even under ideal heat transfer conditions (an isothermal bed assumption). Additionally, a minimal centerline fin-fin spacing for the transverse fin design would present significant manufacturing difficulties when attempting to pack the hydride precursor into the storage vessel between the fins.

3.5.2 Script for the Transverse Fin Model

Initially, a unit cell model for a transverse fin design was built manually within COMSOL®. The material properties, boundary conditions, subdomain equation system were specified as previously described and this model was then exported as a MatLab® file. Thermal contact resistances between boundaries are modeled via a thin, thermally-resistive layer within COMSOL®. The resulting file was modified to make it a MatLab® function taking the aforementioned geometrical parameters as input to build the prescribed geometry, run the model, and return the amount of hydrogen stored as hydride within twelve minutes, the fin volume, the tube volume, and the "fem" variable in which COMSOL® stores the entire model.

An initial mesh was generated for the transverse fin model using the built-in advancing-front triangular mesh method with an 'hauto' setting of '4.' This mesh was then smoothed using the built-in "meshsmooth" function, refined for the subdomains corresponding to the hydride precursor, the "media," and the cooling tube in direct contact with the media, and smoothed again. Since the temperature at most boundaries is not fixed, boundaries between subdomains with "identity pairs" to allow for thermal contact resistances must be meshed exactly the same. Otherwise, small numerical differences in fluxes across the boundaries between subdomains may appear causing heat to be lost (or generated) resulting in unphysical solutions, e.g., temperatures that approach 0 K. Periodic boundary conditions, linking boundaries like the bottom surface of the bottom fin and the top surface of the top fin in this unit cell model, are implemented in COMSOL® as a special case of an extrusion coupling variable. Similarly, the top and bottom boundaries with periodic boundary conditions must be meshed exactly the same. Figure 3 shows a representative mesh that the scripts generate and the corresponding mesh statistics are given in Table 2.

Table 2: Mesh statistics for a finite element mesh generated for a transverse-fin, unit-cell model.

Number of degrees of freedom	13688
Number of mesh points	1448
Number of elements	2434
Triangular	2434
Quadrilateral	0
Number of boundary elements	450
Number of vertex elements	24
Minimum element quality	0.6965
Element volume ratio	0.0806
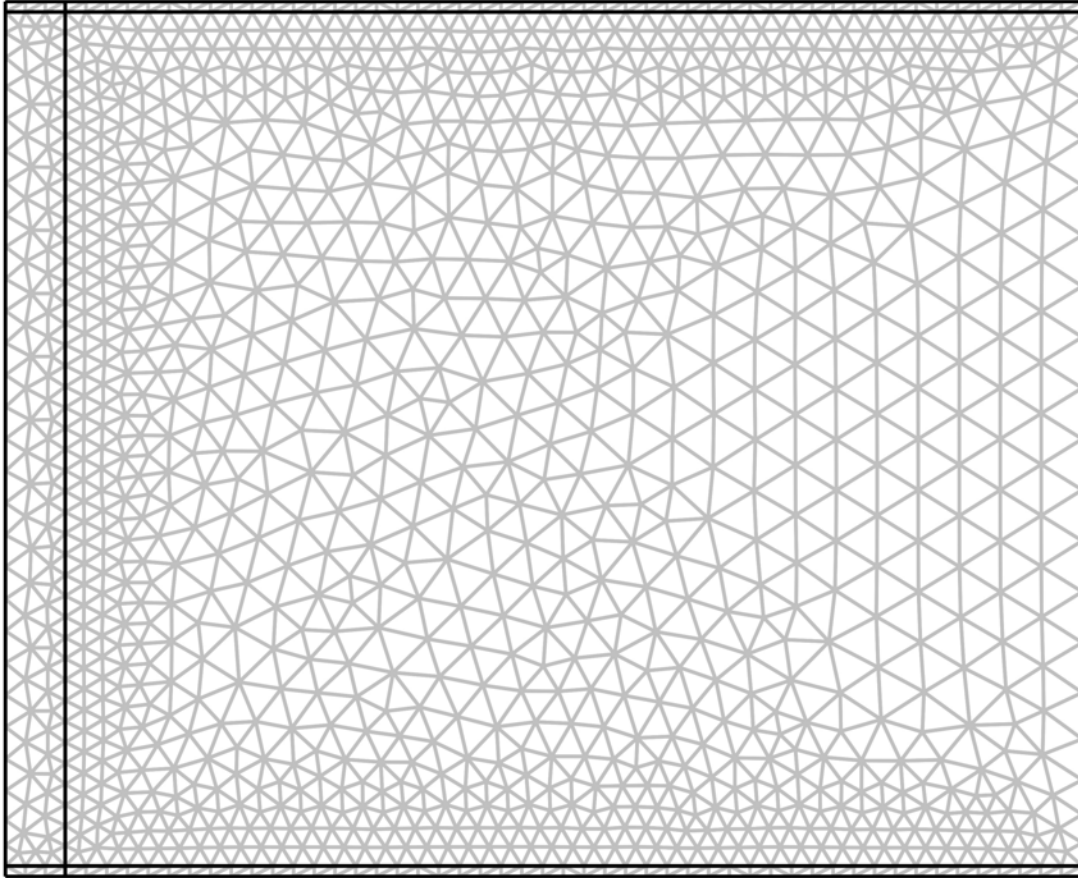
Figure 3: Sample finite element mesh generated for a transverse fin unit cell model.

3.5.3 Script for the Longitudinal Fin Model

Similar to the transverse fin script, a unit cell model for a longitudinal fin design was initially built manually within COMSOL®. The material properties, boundary conditions, subdomain equation system were specified as previously described and this model was then exported as a MatLab® file. The resulting file was modified to make it a MatLab® function taking the aforementioned geometrical parameters as input to build the prescribed geometry, run the model, and returns the follow:

1. The amount of hydrogen stored as hydride over a twelve minute charging time.
2. The fin cross-sectional area and the tube cross-sectional area.
3. The media cross-sectional area.
4. The "fem" variable in which COMSOL® stores the entire model.

The ordering of boundaries and subdomains within COMSOL® complicates the creation of automatic scripts for making general geometrical models of cylindrical (2-dimensional, axisymmetrical) geometries such as those needed in this work. In general, subdomains are ordered from left to right and then from top to bottom based on the leftmost vertex (leftmost and uppermost if two vertices have equal left-right positioning)

of the subdomain. The ordering of the boundaries is a bit more complicated. First, all boundaries of subdomain *n* come before any boundaries of subdomain *n+1*. Second, all boundaries composed of straight lines are ordered before any curved boundaries, which are represented by one or more rational (or weighted) Bezier curves. Finally, the boundaries that come first within each class of boundaries within each subdomain, are those with the leftmost vertex (and uppermost if two vertices have equal left-right positioning). These ordering rules become important if the thickness of a subdomain changes significantly relative to the length of the fin, e.g., the ordering of the boundaries of a cooling fin if the fin length is short and the fin thickness is wide versus long and skinny.

The same concerns about identity pair boundaries and periodic boundaries (boundaries linked via an extrusion coupling variable) that applied to the meshing of a transverse fin model apply to the meshing of a longitudinal fin model. The boundaries lying on constant-θ lines (in an r-θ coordinate system) were meshed first. The boundary between the cooling tube and the hydride precursor media was meshed next. A 'quad' mesh was generated for the subdomains corresponding to the fins and the portions of the cooling tube in direct contact with the fins. This 'quad' mesh was then converted to a triangular mesh using the 'meshconvert' command and smoothed using the 'meshsmooth' command. A mesh was then generated for the remaining subdomain corresponding to the cooling tube and the subdomain corresponding media using the built-in advancing-front triangular mesh method with an 'hauto' setting of '4.' Finally, the complete mesh was smoothed one last time. Figure 4 shows a representative mesh that the scripts generate and the corresponding mesh statistics are given in Table 3.

3.6 Initial Geometrical Scoping

Once the scripts were completed to generate transverse and longitudinal fin models of arbitrary dimensions based on passed parameters, a simple MatLab® script was generated to loop through an initial range of values for the parameters and run simulations for the transverse fin model. The range of parameter values was estimated from previous insight and experience. The three values investigated for each the parameters were as follows:

Internal diameter of the cooling tube:	0.250, 0.375, and 0.500 in.
Thickness of the cooling tube:	0.05, 0.10, and 0.20 in.
Length of cooling fin:	0.25, 0.50, and 1.00 in.
Thickness of the cooling fin:	0.004, 0.010, and 0.020 in.
½ fin-fin centerline spacing:	0.1, 0.2, and 0.4 in.

The 243 simulations that correspond to all possible permutations of the values for these five parameters were run. The number of unit cells required to store 1 kg of H_2 was calculated from each simulation corresponding to a specific combination of parameter values. Based on this number of unit cells, the mass of media and mass of the integrated heat exchanger, i.e., the mass of aluminum in the cooling tubes and fins, were calculated with the results for each run written to a text file. The parameter values corresponding to the minimum system mass for the transverse fin model were assumed to be reasonable

Table 3: Mesh statistics for sample finite element mesh generated for a longitudinal-fin, unit-cell model.

Number of degrees of freedom	7879
Number of mesh points	863
Number of elements	1393
Triangular	1393
Quadrilateral	0
Number of boundary elements	321
Number of vertex elements	24
Minimum element quality	0.6566
Element volume ratio	0.0311
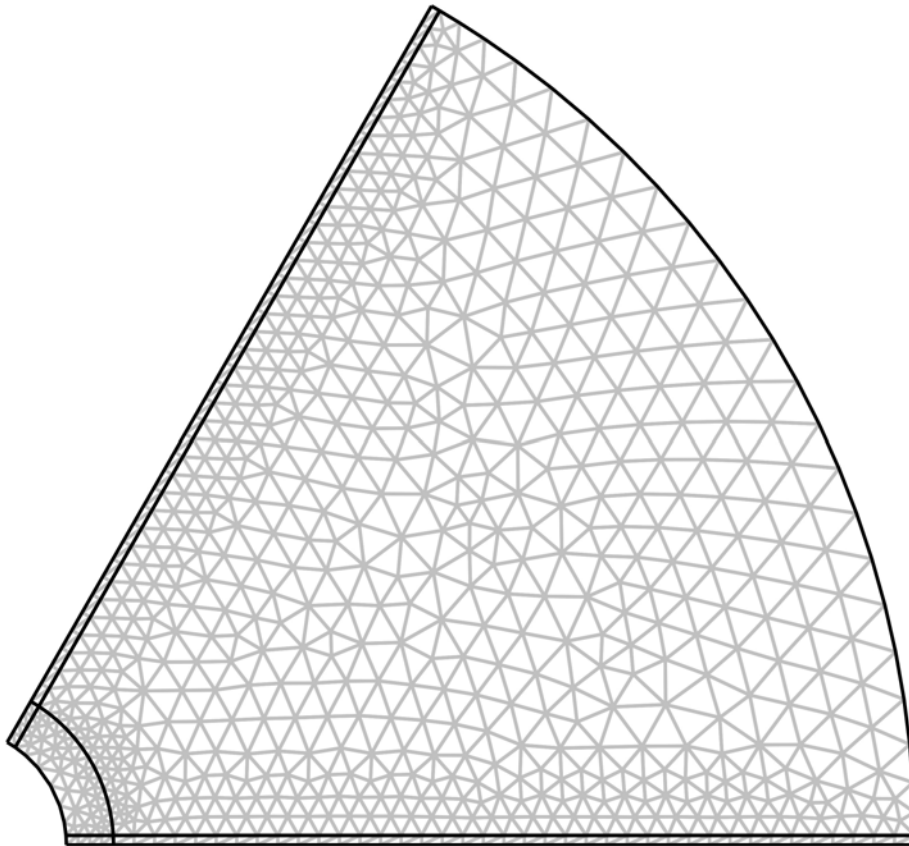
Figure 4: Sample finite element mesh generated for a longitudinal- fin, unit-cell model.

estimates of the parameter values that would yield and minimum system mass for thelongitudinal fin model. As such, they were also used for the initial guess for the optimization of the longitudinal fin model.

3.7 Nelder-Mead Simplex Optimization

In a desire to move beyond the somewhat simplistic optimization scoping described in the previous section, the built-in Nelder-Mead, or downhill-simplex,

optimization heuristic within MatLab® was investigated. The Nelder-Mead method uses a simplex, a polytope with *n+1* vertices in *n* dimensions, to attempt to minimize an objective function in *n*-dimensional parameter space. In this case each vertex would correspond to a set of parameters describing a single model geometry. A simple description of the Nelder-Mead method for a system of two variables (i.e., *n*=2) will be provided here but a more detailed discussion is available elsewhere [16-17]. A simplified schematic of the algorithm is provided in Figure 5.

Before the optimization begins, the function value at three points must be determined. The method starts by ordering these three points based on the objective function, in this case the mass of the storage system internals. Once the points are ordered (Step 0), the algorithm determines the point x_0 that corresponds to the centroid of the 2 best points, and then proceeds to pick a new point, x_r, corresponding to the reflection of the worst point, x_3, through x_0. (This is Step 1.) If x_r is not better than the best point so far (x_1), but it is better than the second worst point (x_2), replace x_3 with x_r and start over at Step 0 with the three new points. If x_r is better than x_1, look at a point, x_e, further down the line from x_0 to x_r to possibly expand the simplex. Then, replace x_3 with the better of x_e and x_r, and start over at Step 0.

If x_r is not better than x_2, try to contract the simplex one of two ways. If x_r is better than x_3 (Case 1), look at the point x_{co} that is located between x_0 and x_r. If x_{co} is better than x_r (and therefore also better than x_3), replace x_3 with x_{co} and start over at Step 0. (This is sometimes referred to as "contract-outside.") If x_{co} is worse than x_r, "shrink" the simplex, which will be discussed shortly. If x_r is worse than x_3 (Case 2), look at the point x_{ci} that is located between x_3 and x_0. If x_{ci} is better than x_3, replace x_3 with x_{ci} and start over at step 0. This is sometimes referred to as "contract-inside." If x_{ci} is worse than x_3, shrink the simplex.

To shrink the simplex, calculate new points (x_{s2} and x_{s3}) between the previous points (x_2 and x_3) and the best point (x_1), replace the old points (x_2 and x_3) with the new points (x_{s2} and x_{s3}), and start over at Step 0. (Note that, for two dimensions, x_{s2} will commonly be the same as x_0.) The entire process is repeated until the size of the simplex shrinks or contracts to some small size.

The Nelder-Mead methodology has several advantages, especially for optimizations based on simulation results. First, gradients and derivatives of the objective function are not needed for the optimization to proceed. Second, unless a shrink step is required, only one new point will be accepted and reordering the points only requires inserting just this newly accepted point into the appropriate position within the list of the already sorted points. Therefore, the computational overhead between cycles is minimal.

A wrapper script was developed to interface the generation and running of a single unit-cell model design and the built-in Nelder-Mead, or downhill-simplex, optimization technique within MatLab®. The built-in Nelder-Mead routine passes a vector of parameters to a function and expects a single value to be returned. However, the model-building scripts use individual parameters and return multiple values. The wrapper script alleviates these two disconnects.

The script takes the amount of hydrogen stored within the given time in a single unit cell and calculates the number of equivalent unit cells required to store 1 kg of hydrogen. Then, using the mass of media, cooling tube, and cooling fins, the total mass of

Figure 5: Schematic of the Nelder-Mead downhill simplex algorithm for an optimization in two dimensions.

the tank internals necessary to store 1 kg of hydrogen can be determined. (The mass of vessel walls, i.e., the tank shell, and the balance of plant was assumed to be close enough to a constant, i.e., independent of the geometrical parameters, that it could be neglected in the optimizations within this initial work.) The Nelder-Mead optimization routine then optimizes the geometrical parameters to minimize this mass required to store 1 kg of hydrogen, which maximizes the gravimetric capacity (media and heat exchanger basis) as each situation stores 1 kg of hydrogen within the media..

The traditional Nelder-Mead method does not constrain the values for the parameters. However, spatial dimensions within the model that are negative or zero are non-sensical and manufacturing would generally limit how small the tubes or fins could be made. Therefore, if the Nelder-Mead routine attempts to request a value outside of the allowed parameter ranges, the value of the parameter actually passed to the model-building script from within the wrapper script is shifted to the minimum (or maximum) allowed value.

Concurrently, an additional weighting proportional to the square of the difference between requested parameter value and the minimum (or maximum) allowed parameter value is applied to the value of the mass (the objective function) calculated by the model-building routine before it is returned to the Nelder-Mead routine from the wrapper script. Specifically, the mass returned to Nelder-Mead routine is equal to the mass calculated with the parameters shifted to the allowed range times one plus the additional weight. (If multiple parameters are outside the allowable range, an additional weight for each is calculated and the total additional weight is their sum total.) The functional form of this extra weighting was chosen to try to make it and its first derivative go to zero smoothly as the requested parameter value approached the minimum (or maximum) allowed parameter value. Therefore, the response surface is first order continuous, but there is a discontinuity in the gradients when crossing the boundaries corresponding to the minimum or maximum allowed parameter value. No models are built and run with parameters outside of the allowed range. The following values, some of which are

smaller than the minimum allowed in the grid-based optimization, were used as minimum allowable values:

Internal diameter of the cooling tube:	0.085 in.
Thickness of the cooling tube:	0.020 in.
Length of cooling fin:	0.250 in.
Thickness of the cooling fin:	0.004 in.
½ fin-fin centerline spacing (transverse fin design):	0.100 in.

No maximum values were specified or enforced.

4   Results and Discussion

Initially, the simulations were run on a Dell Precision M90 with 4GB of RAM and an Intel Core 2 Duo T7400 CPU operating at 2.167 GHz. Each simulation, transverse fin model or longitudinal model, required about 0.5 minutes. Each simplex optimization required on the order of 100 individual simulations. As previously mentioned, each simulation used a unit cell model to estimate the size of the tank internals – hydride precursor, cooling tubes, and cooling fins – required to store 1 kg of hydrogen within 12 minutes at a hydrogen feed pressure of 50 bar and a cooling system temperature of 100 °C (373.15 K).

4.1 Grid or Geometrical Scoping Results

Of the 243 transverse fin configurations studied in the grid scoping calculations, the model configuration with the minimum total mass of 158 kg (130 kg hydride precursor, 28 kg of cooling tubes and cooling fins) and had the following design:

Internal diameter of the cooling tube:	0.250 in.
Thickness of the cooling tube:	0.050 in.
Length of cooling fin:	0.500 in.
Thickness of the cooling fin:	0.004 in.
½ fin-fin centerline spacing:	0.100 in.

Except for the fin length, the optimal parameter values corresponded to the minimum value investigated. This design would require 42195 unit cells corresponding to a linear length, for a single tube, of 703 ft (213 m) in order to store 1 kg of hydrogen within the metal hydride.

Neglecting the fin-fin centerline spacing, which was held at 60°, the parameter values found to result in the minimum total mass for the transverse fin design were found to also result in the longitudinal fin configuration with the minimum total mass. To store 1 kg of hydrogen within the metal hydride, this design would have a total mass of 169 kg and require a linear length of 775 ft. (234 m), e.g., 234 independent cooling tubes in a tank 1 m in length. These tubes would be spaced 1.35 in. (3.4 cm) apart. These parameter values were then used as an initial guesses for the Nelder-Mead simplex optimization for both designs.

4.2 Nelder-Mead Simplex Optimization Results

The Nelder-Mead simplex optimization was initiated using the parameter set from the grid scoping calculations that resulted in the minimum total mass as the initial guess (MatLab® generates the other *n* initial points for the initial simplex based on this one initial point.). With enforcement of the constraints previously mentioned, the minimum mass of the tank internals for the transverse fin design was 141 kg and corresponded to the following design:

Internal diameter of the cooling tube:	0.085 in.
Thickness of the cooling tube:	0.020 in.
Length of cooling fin:	0.290 in.
Thickness of the cooling fin:	0.004 in.
½ fin-fin centerline spacing:	0.146 in.

To store 1 kg of hydrogen within the metal hydride, this design would require approximately 97,800 unit cells with 14.9 kg of aluminum cooling tubes and cooling fins and 126 kg of hydride precursor. This corresponds to a linear length of 2379 ft (719 m) or an internal tank volume of 6.46 ft^3 (0.178 m^3). For the given constraints and feed conditions, this yields a maximum gravimetric density for the tank internals (the "bed") of 0.007 kg H$_2$/kg bed (0.7 wt % H$_2$). (The full storage system gravimetric density would be even lower.) This closely matches the gravimetric capacity of the previous 0-D, isothermal scoping results,[2] indicating that the system is not heat transfer limited.

The Nelder-Mead simplex optimization of the longitudinal fin design results in similar parameters for the optimal design, which is as follows:

Internal diameter of the cooling tube:	0.100 in.
Thickness of the cooling tube:	0.020 in.
Length of cooling fin:	0.340 in.
Thickness of the cooling fin:	0.004 in.

To store 1 kg of hydrogen within the metal hydride, this design would require a linear length of approximately 1777 ft (537 m), e.g., 537 independent cooling tubes in a 1 m long tank vessel, with 14.7 kg of aluminum cooling tubes and cooling fins and 126 kg of hydride precursor. For the given constraints and feed conditions, this yields a maximum gravimetric density of 0.007 kg H$_2$/kg bed (0.7 wt % H$_2$).

Similar to the results of the grid-based scoping calculations, the minimum tank mass configuration corresponds to parameters values near the constrained minimum values. The optimal value of the cooling tube thickness and the cooling fin thickness are at the minimum value allowed for both fin designs. Only the optimal fin lengths, for both designs, the optimal cooling tube diameter for the longitudinal fin model, and the optimal fin-fin centerline spacing for the transverse fin model are larger than the minimum allowed values.

5 Conclusions

The results of the simulations and optimizations point to very small cooling tubes and very small spacing between cooling tubes to maximize the gravimetric capacity of

SRNL-STI-2011-00424

the stored hydrogen, balancing (1) the heat transfer and reaction kinetics with (2) the total system mass. These design parameters are likely to be controlled by their manufacturability such that actual designs may require larger minimum sizes and spacing. The optimal longitudinal fin design appears to be slightly, but likely negligibly, more efficient than the transverse fin design. Both designs require approximately 126 kg of hydride precursor for the conditions studied, with the longitudinal fin design requiring 0.2 kg less metal for the cooling tube and cooling fins (14.7 kg versus 14.9 kg for the longitudinal and transverse fin designs, respectively). As both designs closely match the gravimetric capacity of the previous 0-D, isothermal scoping results, these designs are limited more by the reaction kinetics than by heat transfer issues.

Given the specified hydrogen feed pressure of 50 bar, the kinetics are much too slow to meet the DOE targets. As a rough estimate the fill time must be reduced by a factor of three (from 12 minutes to four minutes) and the stored hydrogen must be increased by at least a factor of eight (from 0.7 to 5.6 wt%, which is somewhat unlikely as it is the maximum theoretically possible for sodium alanate). Combined, these would necessitate increasing the system pressure or finding catalysts to improve the hydrogen uptake kinetics by at least a factor of 24 while simultaneously maintaining an equivalent temperature profile. As such, materials to enhance the thermal conductivity of the bed, e.g., expanded natural graphite, will likely be required to handle the increased heat load generated. Note, however, that these materials would further reduce the actual maximum capacity of the bed in comparison with the maximum theoretical capacity of the hydride precursor.

6 Future Work

The current methodology can be easily extended to new kinetics models for sodium alanate corresponding to improved hydrogen uptake catalysts, to other hydride precursors, or to other hydrogen storage systems, such as cryogenic adsorbents. It would be useful to apply the optimization procedure using the sodium alanate kinetics corresponding to UTRC's $TiCl_3/AlCl_3$ catalyzed sodium alanate [13; 18]. Recent 0-D scoping analysis of the UTRC kinetics of sodium alanate catalyzed with 4% $TiCl_3$ as currently used here indicate hydrogen feed pressures at least above 250 bar would likely be required to satisfy current fill time requirements. Similar 0-D scoping analysis for systems using the UTRC kinetics for sodium alanate catalyzed with $TiCl_3/AlCl_3$ indicate that hydrogen pressures as low as 120 bar may satisfy the same fill times requirements, but at cooling system temperatures closer to 150 °C. Higher hydrogen feed pressures should improve the hydrogen uptake kinetics and the amount of hydrogen stored in the gas phase. As such, experiments and simulations at these higher hydrogen feed pressures should be completed to determine if DOE targets may be reachable at these conditions.

The current models do not account for hydrogen stored in the gas phase within the pores between the precursor particles. For a given temperature and pressure, this should be an additive constant that does not affect the optimization analysis significantly, but would raise the gravimetric capacity of the bed. However, for completeness, the gaseous stored hydrogen should be included in future models as the temperature profiles for each set of design parameters may not be the same, shifting the amount of gas phase hydrogen that is stored. Additionally, explicit modeling of the flow of hydrogen, and possibly the

hydrogen feed tubes, should be included to allow the simulations to model heat transfer requirements and mass transfer capacity under both charging and discharging conditions.

The temperature of the cooling fluid may need to be included as an optimization variable in future studies. The optimal value may be one that is sub-cooled design compared to the 0-D scoping results in order to satisfy DOE targets as an increased hydrogen uptake rate will significantly increase the amount of heat generated. The mass of the pressure vessel should also be included in the optimization as the system geometry, i.e., the tank volume and/or surface area, may change significantly between sets of design parameters. This would require input and research as to what is the maximum allowable length for the tank, commonly accepted tank length to tank diameter ratios, and an effectiveness factor for the hydride precursor media volume versus total tank volume.

References

[1] Targets for Onboard Hydrogen Storage Systems for Light-Duty Vehicles (Rev. 4.0). US Department of Energy Office of Energy Efficiency and Renewable Energy and The FreedomCAR and Fuel Partnership; 2009; http://www1.eere.energy.gov/hydrogenandfuelcells/storage/pdfs/targets_onboard_hydro_ storage_explanation.pdf.

[2] Hardy BJ, Anton DL. Hierarchical methodology for modeling hydrogen storage systems. Part I: Scoping models. Int. J. Hydrog. Energy 2009; 34: 2269-77.

[3] Hardy BJ, Anton DL. Hierarchical methodology for modeling hydrogen storage systems. Part II: Detailed models. Int. J. Hydrog. Energy 2009; 34: 2992-3004.

[4] Mellouli S, Askri F, Dhaou H, Jemni A, Ben Nasrallah S. A novel design of a heat exchanger for a metal-hydrogen reactor. Int. J. Hydrog. Energy 2007; 32: 3501-7.

[5] Mellouli S, Askri F, Dhaou H, Jemni A, Ben Nasrallah S. Numerical study of heat exchanger effects on charge/discharge times of metal-hydrogen storage vessel. Int. J. Hydrog. Energy 2009; 34: 3005-17.

[6] Mellouli S, Askri F, Dhaou H, Jemni A, Ben Nasrallah S. Parametric studies on a metal-hydride cooling system. Int. J. Hydrog. Energy 2009; 34: 3945-52.

[7] Askri F, Salah MB, Jemni A, Ben Nasrallah S. Optimization of hydrogen storage in metal-hydride tanks. Int. J. Hydrog. Energy 2009; 34: 897-905.

[8] Mellouli S, Askri F, Dhaou H, Jemni A, Ben Nasrallah S. Numerical simulation of heat and mass transfer in metal hydride hydrogen storage tanks for fuel cell vehicles. Int. J. Hydrog. Energy 2010; 35: 1693-705.

[9] Kikkinides ES, Georgiadis MC, Stubos AK. On the optimization of hydrogen storage in metal hydride beds. Int. J. Hydrog. Energy 2006; 31: 737-51.

[10] Kikkinides ES, Georgiadis MC, Stubos AK. Dynamic modelling and optimization of hydrogen storage in metal hydride beds. Energy 2006; 31: 2428-46.

[11] MacDonald BD, Rowe AM. Impacts of external heat transfer enhancements on metal hydride storage tanks. Int. J. Hydrog. Energy 2006; 31: 1721-31.

[12] Mohan G, Maiya MP, Murthy SS. Performance simulation of metal hydride hydrogen storage device with embedded filters and heat exchanger tubes. Int. J. Hydrog. Energy 2007; 32: 4978-87.

[13] Mosher DA, Tang X, Brown RJ, Arsenault S, Saitta S, Laube BL, et al. High Density Hydrogen Storage System Demonstration Using NaAlH4 Based Complex Compound Hydrides. East Hartford (CT): United Technologies Research Center; 2007. Report No.: DOE/AL/67610.

[14] Bogdanović B, Brand RA, Marjanović A, Schwickardi M, Tölle J. Metal-doped sodium aluminium hydrides as potential new hydrogen storage materials. Journal of Alloys and Compounds 2000; 302: 36-58.

[15] Thomas GJ, Guthrie SE, Gross K, Hydride development for hydrogen storage, in: Proceedings of the 1999 U.S. DOE Hydrogen Program Review, NREL/CP-570-26938.

[16] Nelder JA, Mead R. A simplex-method for function minimization. Comput. J. 1965; 7: 308-13.

[17] Lagarias JC, Reeds JA, Wright MH, Wright PE. Convergence properties of the Nelder-Mead simplex method in low dimensions. SIAM J. Optim. 1998; 9: 112-47.

[18] Mosher D, Tang X, Arsenault S, Laube B, Cao M, Brown R, et al., High Density Hydrogen Storage System Demonstration Using NaAlH$_4$ Complex Compound Hydrides, in: Proceedings of the 2002 U.S. DOE Hydrogen Program Review.